Systematic study of multifragmentation in asymmetric colliding nuclei

Varinderjit Kaur and Suneel Kumar[*]

School of Physics and Material Science, Thapar University, Patiala 147004, Punjab, India
(Received 3 April 2010; published 22 June 2010)

We present a complete systematically theoretical study of multifragmentation for asymmetric colliding nuclei for heavy-ion reactions in the energy range between 50 MeV/nucleon and 600 MeV/nucleon by using soft and hard equations of state. This study is performed within an isospin-dependent quantum-molecular dynamics model. To see the effect of mass asymmetry, simulations are carried out in the absence of Coulomb interactions. Coulomb interactions enhance the production of fragments by about 20%. We envision an interesting outcome for large asymmetric colliding nuclei. Although nearly symmetric nuclei depict a well-known trend for rising and falling with a peak around $E = 100$ MeV/nucleon, this trend, however, is completely missing for large asymmetric nuclei. Therefore, experiments are needed to verify this prediction.

I. INTRODUCTION

The ability to understand the properties of nuclear matter at the extreme conditions of temperature and density is one of the challenges in present-day nuclear-physics research. Such extreme conditions can be generated in a heavy-ion-induced reaction at intermediate energies [1,2]. The outcome of a reaction depends on the incident energy, the impact parameter, as well as on the asymmetry of the colliding partners [1–5]. For symmetrically heavy colliding nuclei at central impact parameters, two primary fragments are formed: one that is the projectilelike fragment and the other that is the targetlike fragment. These excited fragments deexcite through various exit channels: evaporation of light particles and emission of intermediate-mass fragments (IMFs) [1–5]. The excitation energy deposited in the system at low incident energies is too small to allow the break up of the nuclei into fragments. With an increase in the incident energy, colliding nuclei may break into dozens of fragments consisting of light, medium, and heavy fragments. The size of the fragments and physics behind their formation differs in different physical conditions. No such fragments will survive at extremely high incident energies.

Among various theoretical models developed to study these reactions, one can group them into those, which are statistical in nature [6], and others, which take the dynamics of the reaction into account and, hence, are capable of investigating the evolution of the fragmentation and nucleon-nucleon correlations [1–5,7,8]. Interestingly, both types of models (although different in their assumptions) are able to explain one or the other feature of the experimental findings. Here, we will only concentrate on the dynamical model. A careful analysis of experimental efforts reveals either that one has studied the collision of symmetric nuclei (e.g., $_{79}Au^{197} + _{79}Au^{197}$) [3] or that one has studied asymmetric colliding nuclei (e.g., $_{20}Ar^{40} + _{21}Sc^{45}$, $_{20}Ar^{40} + _{79}Au^{197}$, $_6C^{12} + _{79}Au^{197}$, $_{20}Ca^{40} + _{79}Au^{197}$) [3]. Although the dynamics for symmetrically heavy nuclei is prominently exposed in experimental and theoretical

studies, little attention is paid to the collision of asymmetric nuclei. We, at the same time, know that the symmetry and the isospin play decisive roles in a reaction. We want to discover the fragmentation of asymmetrically colliding pairs in the following different ways. (i) In the first case, we will perform a systematic study of the emission of various fragments as a function of the asymmetry η of a reaction. The asymmetry of a reaction can be defined by the asymmetry parameter $\eta = (A_T - A_P)/(A_T + A_P)$ [9,10]; A_T and A_P are, respectively, the masses of the target and the projectile. $\eta = 0$ corresponds to the symmetric reaction, whereas nonzero values of η define different asymmetries of the reaction. It is worth mentioning that the outcome and the physical mechanism behind the symmetric and asymmetric reactions are entirely different [3,9,10]. Here, for systematic analysis, we start from the symmetrically colliding partners ($\eta = 0$), and then, asymmetry parameter η is varied gradually ($\eta = -0.8$–0.8) by keeping the total mass of the system fixed. Such an experiment was performed by Betts [11] in 1981, where fusion probabilities were measured for different colliding pairs, which led to the same compound nucleus. (ii) In the second case, the projectile mass is varied from 16 to 56 units, while the total mass of the system is kept fixed. For example, we study the reactions of $_8O^{16} + _{54}Xe^{136}$, $_{14}Si^{28} + _{54}Xe^{124}$, $_{16}S^{32} + _{50}Sn^{120}$, $_{20}Ca^{40} + _{50}Sn^{112}$, $_{24}Cr^{50} + _{44}Ru^{102}$, $_{26}Fe^{56} + _{44}Ru^{96}$, etc. The target isotope is chosen to be a stable one. Since we will neglect the Coulomb effect, we may say that it leads to the same compound nucleus.

In a recent communication [12], Liu studied the isospin effects on the process of multifragmentation and dissipation by considering the two pairs of colliding systems $Zn^{76} + Ar^{40}$ and $Kr^{76} + Ca^{40}$ and $Cd^{120} + Ar^{40}$ and $Xe^{120} + Ca^{40}$ for central collisions. Another study [12] focused on the isospin effects of the mean-field and two-body collisions on nucleon emissions at intermediate energies. This study showed that the neutron-proton ratio of preequilibrium nucleon emission and the neutron-proton differential and elliptical flows are the probes for extracting the isospin-dependent mean field at a lower beam-energy region. Because of less compression in asymmetric reactions, most of the deposited excitation energy is in the form of thermal energy. Our present study will shed

---

*suneel.kumar@thapar.edu

some light on the effect of the asymmetry of a reaction on fragmentation, where a great amount of energy is in the form of thermal energy.

The present analysis will be carried out within the framework of the isospin-dependent quantum-molecular dynamics (IQMD) model [2,13]. Our paper is organized as follows: We briefly discuss the model in Sec. II. Our results are given in Sec. III, and we summarize the results in Sec. IV.

II. THE MODEL

The IQMD [2] model treats different charge states of nucleons, deltas, and pions explicitly [14], as shown in the Vlasov-Uehling-Uhlenbeck (VUU) model [15]. The IQMD model was successfully used in analyzing the large number of observables from low to relativistic energies [2,4,5,13–15]. One of its versions (quantum-molecular dynamics) has been very successful in explaining the subthreshold particle production [16], the multifragmentation [4,8], the collective flow [4,17], the disappearance of flow [17], and the density temperature reached in a reaction [8]. We will not take relativistic effects into account, since there is no effect [18] in the energy domain in which we are interested. The isospin degree of freedom enters into the calculations via both cross sections and mean field [15]. The details about the elastic and

inelastic cross sections for proton-proton and neutron-neutron collisions can be found in Refs. [2,18].

In this model, baryons are represented by Gaussian-shaped density distributions,

$$f_i(r, p, t) = \frac{1}{\pi^2 \hbar^2} \exp \frac{-[r - r_i(t)]^2}{2L} \exp \frac{-[p - p_i(t)]^2 \cdot 2L}{\hbar^2}.$$

$$(1)$$

Nucleons are initialized in a sphere with radius $R = 1.12 A^{1/3}$ fm, in accordance with the liquid-drop model. Each nucleon occupies a volume of $\hbar^3$ so that phase space is uniformly filled. The initial momenta are randomly chosen between 0 and Fermi momentum p_F. The nucleons of the target and the projectile interact via two- and three-body Skyrme forces and the Yukawa potential. The isospin degrees of freedom are treated explicitly by employing a symmetry potential and the explicit Coulomb forces between protons of the colliding target and protons of the projectile. This helps to achieve the correct distribution of protons and neutrons within the nucleus.

The hadrons propagate by using Hamiltonian equations of motion:

$$\frac{d\vec{r}_i}{dt} = \frac{d\langle H \rangle}{d\vec{p}_i}, \qquad \frac{d\vec{p}_i}{dt} = -\frac{d\langle H \rangle}{d\vec{r}_i}. \qquad (2)$$

with $\langle H \rangle = \langle T \rangle + \langle V \rangle$ as the Hamiltonian

$$= \sum_i \frac{p_i^2}{2m_i} + \sum_i \sum_{j>i} \int f_i(\vec{r}, \vec{p}, t) V^{ij}(\vec{r}', \vec{r}) f_j(\vec{r}', \vec{p}', t) d\vec{r} d\vec{r}' d\vec{p} d\vec{p}'. \qquad (3)$$

The baryon-baryon potential V^{ij}, in the preceding relation, reads as

$$V^{ij}(\vec{r}' - \vec{r}) = V^{ij}_{\text{Skyrme}} + V^{ij}_{\text{Yukawa}} + V^{ij}_{\text{Coulomb}} + V^{ij}_{\text{Sym}}$$

$$= t_1 \delta(\vec{r}' - \vec{r}) + t_2 \delta(\vec{r}' - \vec{r}) \rho^{\gamma-1} \left(\frac{\vec{r}' + \vec{r}}{2} \right)$$

$$+ t_3 \frac{\exp(|\vec{r}' - \vec{r}|/\mu)}{(|\vec{r}' - \vec{r}|/\mu)} + \frac{Z_i Z_j e^2}{|\vec{r}' - \vec{r}|}$$

$$+ t_4 \frac{1}{\rho_o} T_3^i T_3^j \cdot \delta(\vec{r}'_i - \vec{r}_j), \qquad (4)$$

where $\mu = 0.4$ fm, $t_3 = -6.66$ MeV, and $t_4 = 100$ MeV. The values of t_1 and t_2 depend on the values of α, β, and γ [1]. Here, Z_i and Z_j denote the charges of the ith and j^{th} baryons, and T_3^i, T_3^j are their respective T_3 components (i.e., $1/2$ for protons and $-1/2$ for neutrons). The Meson potential only consists of the Coulomb interaction. The parameters μ and $t_1, \ldots, t_4$ are adjusted to the real part of the nucleonic optical potential. For the density dependence of the nucleon optical potential, standard Skyrme-type parametrizations are employed. The Skyrme energy density has been shown to be very successful at low incident energies, where fusion is the dominant channel

[9,10]. The Yukawa term is quite similar to the surface-energy coefficient used in the calculations of the nuclear potential for fusion [19]. The choice of the equations of state (EOS) (or compressibility) is still a controversial one. Many studies advocate softer matter, whereas, a greater number of studies indicate matter to be harder in nature [15,17]. We will use both hard (H) and soft (S) EOS that have compressibilities of 380 and 200 MeV, respectively.

The symmetry energy is taken into account by introducing

$$V^{ij}_{\text{sym}} = t_4 \frac{1}{\rho_o} T_3^i T_3^j \cdot \delta(\vec{r}'_i - \vec{r}_j). \qquad (5)$$

The binary nucleon-nucleon collisions are included by employing the collision term of the well-known VUU-Boltzmann-Uehling-Uhlenbeck equation [15,20]. The binary collisions are allowed stochastically, in a similar manner as performed in all transport models. During the propagation, two nucleons are supposed to suffer a binary collision if the distance between their centroids is,

$$|r_i - r_j| \leqslant \sqrt{\frac{\sigma_{\text{tot}}}{\pi}}, \qquad \sigma_{\text{tot}} = \sigma(\sqrt{s}, \text{type}), \qquad (6)$$

where type denotes the in-going collision partners (N-N, N-δ, N-π,...). In addition, Pauli blocking (of the final

state) of baryons is taken into account by checking the phase-space densities in the final states. The final phase-space fractions P_1 and P_2, which are already occupied by other nucleons, are determined for each of the scattering baryons. The collision is then blocked with probability

$$P_{\text{block}} = 1 - (1 - P_1)(1 - P_2). \qquad (7)$$

The delta decays are checked in an analogous fashion with respect to the phase space of the resulting nucleons.

III. RESULTS AND DISCUSSION

In the present calculations, a simple spatial clusterization algorithm dubbed as minimum-spanning-tree method is used to clusterize the phase space [1]. We, however, also acknowledge that more microscopic algorithmic routines are also available in literature [2,5]. By using the asymmetric (colliding) nuclei, the effect of mass asymmetry can be analyzed without varying the total mass of the system. As noted previously, the experimental studies by the Michigan State University (MSU), miniball and ALADiN Collaboration [21] groups vary the asymmetry of the reaction, whereas the plastic ball and FOPI experiments [22] are only performed for symmetric reactions.

The effect of mass asymmetry on fragmentation is demonstrated in Fig. 1. Here, relative multiplicity R_M is defined as $= |\frac{(M_A - M_S)}{M_S}|$, where M_A and M_S are the multiplicities of various fragments obtained in the asymmetric and symmetric colliding nuclei, respectively. The relative multiplicity of free nucleons, light-mass fragments (LMFs) ($2 \leqslant A \leqslant 4$), medium-mass fragments (MMFs) ($3 \leqslant A \leqslant 8$), and IMFs ($5 \leqslant A \leqslant A_{\text{tot}}/6$) follows hyperbolic behavior. Here, the total mass was kept fixed at 140 units, and the mass of the target and the projectile was varied in steps of 10 units (e.g., $A_P = 130$, $A_T = 10$, $A_P = 120$, $A_T = 20$, etc.). As asymmetry η shifts toward the positive side, the target fragmentation takes place
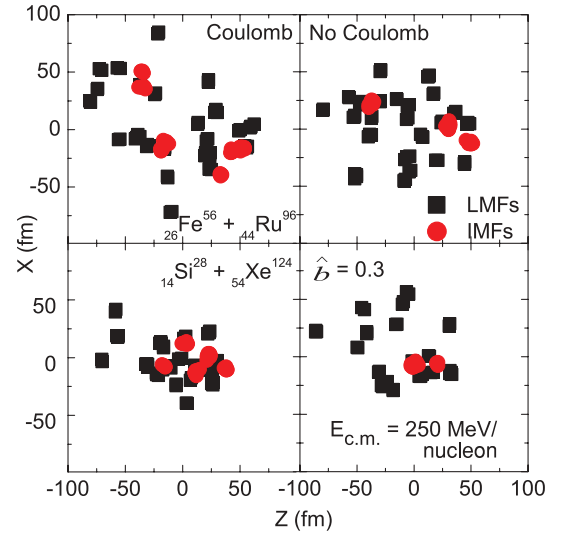
FIG. 2. (Color online) The final-state phase space of a single event for the reaction of $_{26}Fe^{56} + _{44}Ru^{96}$ with and without the Coulomb effects. Here, center-of-mass energy is $E_{\text{c.m.}} = 250$ MeV/nucleon and impact parameter is $\hat{b} = 0.3$. Different symbols denote LMFs and IMFs.

since $A_T \gg A_P$. In contrast, at $\eta = -0.8$, the projectile fragmentation takes place since $A_P \gg A_T$. Since the emission of the nucleons (protons and neutrons) is maximum in the participant zone, one sees less nucleon emission compared to the emission of lighter fragments such as LMFs and MMFs. In this study, all reactions are performed in the laboratory frame. Note that the mirror reactions are also studied by the FOPI collaboration [23].

Now, we confine our study to particular asymmetric systems such as $_8O^{16} + _{54}Xe^{136}$, $_{14}Si^{28} + _{54}Xe^{124}$, $_{16}S^{32} + _{50}Sn^{120}$, $_{20}Ca^{40} + _{50}Sn^{112}$, $_{24}Cr^{50} + _{44}Ru^{102}$, and $_{26}Fe^{56} + _{44}Ru^{96}$ at different incident energies. To see the effect of the Coulomb interactions, in Fig. 2, we display the final phase space of a single event of $_{26}Fe^{56} + _{44}Ru^{96}$ ($\eta = 0.2$) (upper panel) and $_{14}Si^{28} + _{54}Xe^{124}$ ($\eta = 0.6$) (lower panel) at a fixed center-of-mass energy of 250 MeV/nucleon with and without the Coulomb interaction. Here, the phase space of LMFs ($2 \leqslant A \leqslant 4$) and IMFs ($5 \leqslant A \leqslant A_{\text{tot}}/6$) is displayed. Irrespective of the Coulomb interaction, the reaction with $\eta = 0.2$ leads to isotropic emission compared to the reaction with $\eta = 0.6$ that projects a nearly binary character. Since LMFs originate from the midrapidity region, they are better suited for studying the effect of asymmetry on the reaction dynamics.

Generally, obvious effects associated with the asymmetry of a reaction are caused by the Coulomb interaction. To understand the role of asymmetry beyond the Coulomb effects, we switch off the Coulomb force in further analysis. Additionally, we keep the center-of-mass energy fixed throughout the analysis.

In Fig. 3, we compare the effect of the Coulomb forces on the multiplicities of various fragments at $E_{\text{c.m.}} = 50$ MeV/nucleon and $E_{\text{c.m.}} = 250$ MeV/nucleon. The asymmetry of the reaction is varied by using projectiles with masses between 16 and 56. We see a clear effect of the Coulomb forces. As expected, it is maximum for the low incident energies,
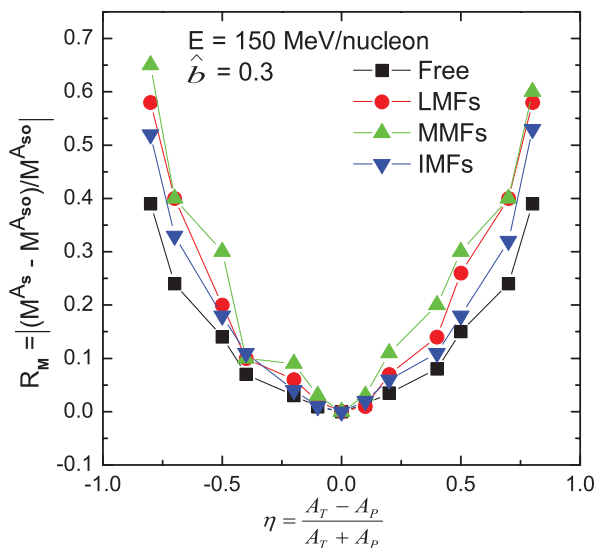

FIG. 1. (Color online) The relative multiplicity of different fragments as a function of mass asymmetry η at $E = 150$ MeV/nucleon and impact parameter at $\hat{b} = 0.3$.
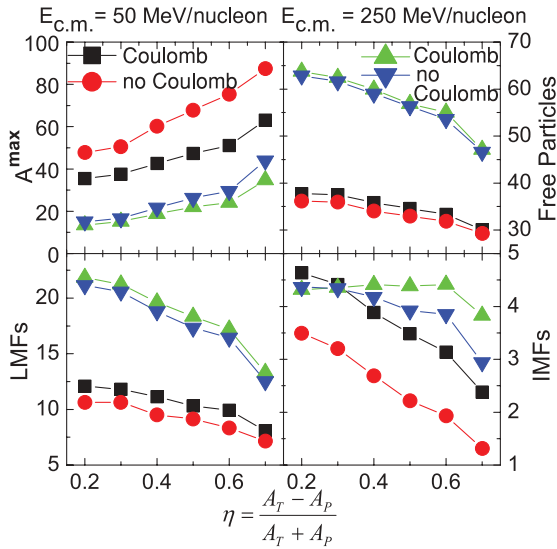
FIG. 3. (Color online) The mass asymmetric η variation of the production of A_{max}, free nucleons, LMFs, and IMFs with and without the Coulomb effect at two different energies at $E_{c.m.} = 50$ MeV/nucleon and $E_{c.m.} = 250$ MeV/nucleon and impact parameter at $\hat{b} = 0.3$.

and this effect diminishes as we move toward higher incident energies. An enhanced effect emerges at larger asymmetric reactions.

Production of the heaviest fragment A_{max}, the free nucleons, the LMFs ($2 \leqslant A \leqslant 4$), and the IMFs ($5 \leqslant A \leqslant A_{tot}/6$) shows expected behavior. The heavier mass continues to grow, and it is close to the mass of the reacting partners for larger asymmetries. In contrast, the production of free nucleons, LMFs, and IMFs shows a reverse trend with the asymmetry of the reaction. This happens because of a decrease in the
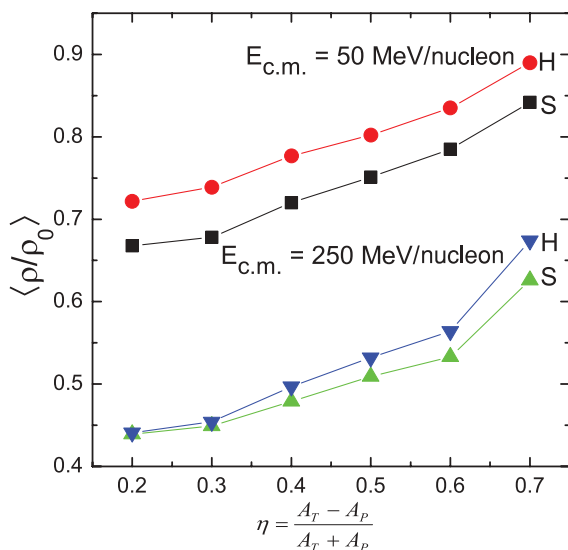

FIG. 4. (Color online) The variation of density with mass asymmetry at an impact parameter $\hat{b} = 0.3$. The different symbols are at $E_{c.m.} = 50$ MeV/nucleon and $E_{c.m.} = 250$ MeV/nucleon with S and H EOS.
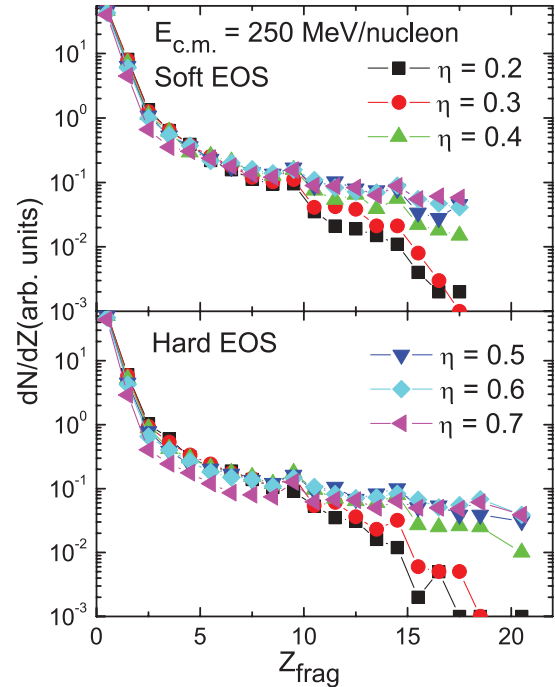

FIG. 5. (Color online) The charge distribution for different asymmetries between $\eta = 0.2$ and 0.7 at $E_{c.m.} = 150$ MeV/nucleon and impact parameter at $\hat{b} = 0.3$. The upper and lower panels are shown with S and H EOS, respectively.

participant zone. Although the role of the Coulomb interaction decreases with energy, its effect, however, remains constant (20%) with the asymmetry of the reaction. Because of the presence of the Coulomb forces, the nuclear matter breaks into smaller pieces/free nucleons.

To understand this aspect further, in Fig. 4, we display the saturation density of the reaction obtained at 200 fm/c. This density remains quite high for larger asymmetries. This is caused by the least amount of destruction of nuclear matter at larger asymmetries, which leads to higher nucleonic densities. As a result, one sees a heavier A_{max} compared to the smaller η values. Because of the heavier A_{max}, the emission of the nucleons is also smaller.

In Fig. 5, the charge distribution is displayed as a function of the fragment charge using S (upper panel) and H EOS (lower panel). The symmetric reactions ($\eta = 0$) lead to enhanced emission of nucleons and LMFs compared to asymmetric reactions, where incomplete fusion events or deep inelastic events are dominant. We can also say that a large asymmetric reaction leads to few nucleonic-transfer processes. One also notices that the slope of the distribution becomes steeper with H EOS compared to S EOS. Because of the enhanced binary collisions between the nucleons for nearly symmetric nuclei, the emission of fragments is suppressed. Clear systematics can be seen in the production of fragments with the asymmetry of the reaction.

In Fig. 6, the variation of the multiplicity of LMFs is displayed as a function of the center-of-mass energy for various asymmetric reactions using H and S EOS. Because of more compression, the nearly symmetric reaction drives matter into
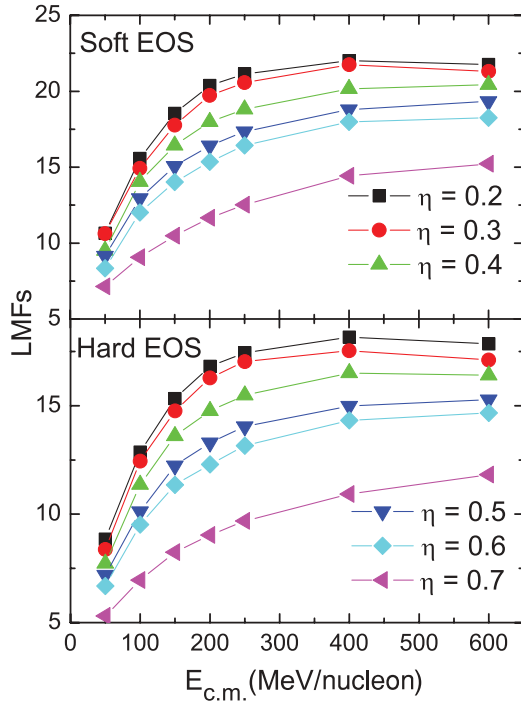
FIG. 6. (Color online) The variation of LMFs with center-of-mass energy using S and H EOS at impact parameter $\hat{b} = 0.3$. The different symbols show the results, which involve different asymmetries.

FIG. 7. (Color online) Same as Fig. 6, but for IMFs.

the participant zone and, as a result, more lighter fragments are emitted.

In Fig. 7, the variation of the multiplicity of IMFs is displayed as a function of the center-of-mass energy $E_{c.m.}$. This happens because of the fact that the system suffers less compression; and, hence, less numbers of IMFs are produced. One notices several interesting points: The nearly symmetric collision leads to a well-known trend (i.e., the maximum emission occurs around 100 MeV/nucleon). This trend, however, is not shown by the large asymmetric reactions, where we do not see any sharp rise or fall; and, furthermore, a flat plateau is obtained at much higher incident energies compared to nearly symmetric nuclei. Therefore, experiments are needed to verify this prediction.
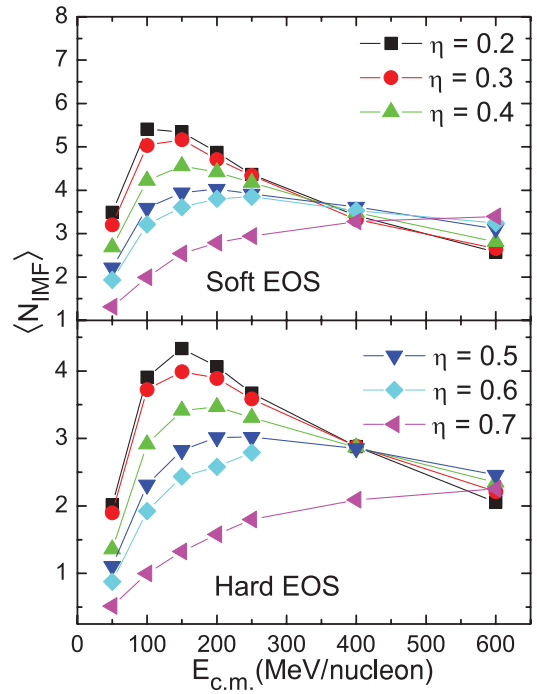
IV. CONCLUSION

A systematically theoretical study is presented for the asymmetric colliding nuclei, which use a variety of reactions that employ different EOS as well as incident energies. We envision an interesting outcome for large asymmetric colliding nuclei, although nearly symmetric nuclei depict a well-known trend of rising and falling with a peak around $E = 100$ MeV/nucleon. This trend, however, is completely missing for large asymmetric nuclei. In conclusion, experiments are needed to verify this prediction.

ACKNOWLEDGMENT

[1] J. Aichelin and H. Stocker, Phys. Lett. B **176**, 14 (1986); J. Aichelin, Phys. Rep. **202**, 233 (1991); W. Cassing, W. Metag, U. Mosel, and K. Nitta, *ibid.* **188**, 363 (1990); G. F. Bertsch and S. Das Gupta, *ibid.* **160**, 189 (1988); H. Feldmeier, Nucl. Phys. A **515**, 147 (1990); J. Schnack, Ph.D. thesis, GSI report, Technische Universität Darmstadt (1996); A. Ono, H. Horiuchi, and T. Maruyama, Phys. Rev. C **48**, 2946 (1993); A. Ono, H. Horiuchi, T. Maruyama, and A. Ohnishi, *ibid.* **47**, 2652 (1993); S. A. Bass, C. Hartnack, H. Stocker, and W. Greiner, *ibid.* **51**, 3343 (1995); B. J. VerWest and R. A. Arndt, *ibid.* **25**, 1979 (1982); B. Jakobsson *et al.*, Nucl. Phys. A **509**, 195 (1990); H. W. Barz *et al.*, *ibid.* **548**, 427 (1992).

[2] C. Hartnack, R. K. Puri, J. Aichelin, J. Konopka, S. A. Bass, H. Stocker, and W. Greiner, Eur. Phys. J. A **1**, 151 (1998); L. Zhuxia, C. Hartnack, H. Stöcker, and W. Greiner, Phys. Rev. C **44**, 824 (1991); P. B. Gossiaux, R. K. Puri, C. Hartnack, and

J. Aichelin, Nucl. Phys. A **619**, 379 (1997); S. Kumar and R. K. Puri, Phys. Rev. C **58**, 320 (1998); **58**, 2858 (1998); **60**, 054607 (1999).

[3] C. A. Ogilvie *et al.*, Phys. Rev. Lett. **67**, 1214 (1991); M. B. Tsang *et al.*, *ibid.* **71**, 1502 (1993); R. T. de Souza *et al.*, Phys. Lett. B **268**, 6 (1991); C. Williams *et al.*, Phys. Rev. C **55**, R2132 (1997); N. T. B. Stone *et al.*, Phys. Rev. Lett. **78**, 2084 (1997); J. Hubble *et al.*, Z. Phys. A **340**, 263 (1991); W. J. Llope *et al.*, Phys. Rev. C **51**, 1325 (1995); T. Rubehn *et al.*, *ibid.* **53**, 993 (1996).

[4] S. Kumar, M. K. Sharma, R. K. Puri, K. P. Singh, and I. M. Govil, Phys. Rev. C **58**, 3494 (1998); S. Kumar, R. K. Puri, and J. Aichelin, *ibid.* **58**, 1618 (1998); S. Kumar, S. Kumar, and R. K. Puri, *ibid.* **78**, 064602 (2008); **81**, 014601 (2010); J. K. Dhawan and R. K. Puri, *ibid.* **75**, 057601 (2007); **75**, 057901 (2007).

[5] R. K. Puri, Ch. Hartnack, and J. Aichelin, Phys. Rev. C **54**, R28 (1996); R. K. Puri and J. Aichelin, J. Comput. Phys. **162**, 245 (2000); Y. K. Vermani, J. K. Dhawan, S. Goyal, R. K. Puri, and J. Aichelin, J. Phys. G **37**, 015105 (2010); Y. K. Vermani and R. K. Puri, Europhys. Lett. **85**, 62001 (2009); Y. K. Vermani, S. Goyal, and R. K. Puri, Phys. Rev. C **79**, 064613 (2009).

[6] J. P. Bondorf *et al.*, Nucl. Phys. A **443**, 321 (1985); D. H. E. Gross, Phys. Prog. Rep. **53**, 605 (1990); A. Botvina *et al.*, Z. Phys. A **345**, 297 (1993).

[7] B. A. Li and D. H. E. Gross, Nucl. Phys. A **554**, 257 (1993); H. M. Xu, C. A. Gagliardi, R. E. Tribble, and C. Y. Wong, *ibid.* **569**, 575 (1994); F. Daffin, K. Haglin, and W. Bauer, Phys. Rev. C **54**, 1375 (1996); V. de la Mota, F. Sebille, M. Farine, B. Remaud and P. Schuck, *ibid.* **46**, 677 (1992).

[8] C. Fuchs, E. Lehmann, R. K. Puri, L. Sehn, A. Faessler, and H. H. Wolter, J. Phys. G **22**, 131 (1996); Y. K. Vermani and R. K. Puri, *ibid.* **36**, 105103 (2009); R. K. Puri, N. Ohtsuka, E. Lehmann, A. Faessler, M. A. Matin, D. T. Khoa, G. Batko, and S. W. Huang, Nucl. Phys. A **575**, 733 (1994); A. D. Sood and R. K. Puri, Phys. Rev. C **79**, 064618 (2009).

[9] R. K. Puri and N. Dhiman, Eur. Phys. J. A **23**, 429 (2005); R. Arora, R. K. Puri, and R. K. Gupta, *ibid.* **8**, 103 (2000); R. K. Puri, M. K. Sharma, and R. K. Gupta, *ibid.* **3**, 277 (1998); R. K. Puri and R. K. Gupta, Phys. Rev. C **51**, 1568 (1995); **45**, 1837 (1992); R. K. Puri, P. Chattopadhyay, and R. K. Gupta, *ibid.* **43**, 315 (1991); R. K. Puri and R. K. Gupta, J. Phys. G **18**, 903 (1992).

[10] R. K. Gupta, S. Singh, R. K. Puri, and W. Scheid, Phys. Rev. C **47**, 561 (1993); R. K. Gupta, S. Singh, R. K. Puri, A. Sandulescu, W. Greiner, and W. Scheid, J. Phys. G **18**, 1533 (1992); S. S. Malik, S. Singh, R. K. Puri, S. Kumar, and R. K. Gupta, Pramana, J. Phys. **32**, 419 (1989); R. K. Puri, S. S. Malik, and R. K. Gupta, Europhys. Lett. **9**, 767 (1989).

[11] R. R. Betts, in *Proceedings for the Conference on Resonances in Heavy Ion Reactions*, edited by K. A. Eberhardt, Lecture Notes in Physics Vol. 156 (Springer, Berlin, 1981), p. 185.

[12] J.-Y. Liu, Y.-F. Yang, W. Zuo, S.-J. Wang, Q. Zhao, W.-J. Guo, and B. Chen, Phys. Rev. C **63**, 054612 (2001); J. Y. Liu, Y. Z. Xing, and W. J. Guo, Chin. Phys. Lett. **20**, 643 (2003).

[13] S. Kumar, S. Kumar, and R. K. Puri, Phys. Rev. C **81**, 014611 (2010).

[14] C. Hartnack, H. Oeschler, and J. Aichelin, Phys. Rev. Lett. **90**, 102302 (2003); J. Phys. G **35**, 044021 (2008).

[15] H. Kruse, B. V. Jacak, and H. Stocker, Phys. Rev. Lett. **54**, 289 (1985); J. J. Molitoris and H. Stocker, Phys. Rev. C **32**, 346(R) (1985); J. Aichelin and G. Bertsch, *ibid.* **31**, 1730 (1985); C. Hartnack, H. Oeschler, and J. Aichelin, Phys. Rev. Lett. **96**, 012302 (2006); A. D. Sood and R. K. Puri, Phys. Rev. C **69**, 054612 (2004); **73**, 067602 (2006); G. D. Westfall *et al.*, Phys. Rev. Lett. **71**, 1986 (1993); D. J. Magestro, W. Bauer, and G. D. Westfall, Phys. Rev. C **62**, 041603(R) (2000).

[16] S. W. Huang *et al.*, Prog. Part. Nucl. Phys. **30**, 105 (1993); G. Batko *et al.*, J. Phys. G **20**, 461 (1994).

[17] A. D. Sood and R. K. Puri, Phys. Rev. C **70**, 034611 (2004); Phys. Lett. B **594**, 260 (2004); E. Lehmann, A. Faessler, J. Zipprich, R. K. Puri, and S. W. Huang, Z. Phys. A **355**, 55 (1996).

[18] E. Lehmann, R. K. Puri, A. Faessler, G. Batko, and S. W. Huang, Phys. Rev. C **51**, 2113 (1995); Prog. Part. Nucl. Phys. **30**, 219 (1993).

[19] I. Dutt and R. K. Puri, Phys. Rev. C **81**, 047601 (2010); **81**, 044615 (2010).

[20] H. Stocker and W. Greiner, Phys. Rep. **137**, 277 (1986); A. D. Sood and R. K. Puri, Phys. Rev. C **69**, 054612 (2004); D. J. Magestro, W. Bauer, O. Bjarki, J. D. Crispin, M. L. Miller, M. B. Tonjes, A. M. VanderMolen, G. D. Westfall, R. Pak, and E. Norbeck, *ibid.* **61**, 021602 (R) (2000); P. Danielewicz, R. Lacey, and W. G. Lynch, Science **298**, 1592 (2002).

[21] D. R. Bowman *et al.*, Phys. Rev. C **46**, 1834 (1992); A. Le Fevre *et al.*, Nucl. Phys. A **735**, 219 (2004); J. Lukasik *et al.*, Phys. Lett. B **566**, 76 (2003); K. Turzo *et al.*, Eur. Phys. J. A **21**, 293 (2004); C. Volant *et al.*, Nucl. Phys. A **734**, 545 (2004); A. Schüttauf *et al.*, *ibid.* **607**, 457 (1996); J. Hubele *et al.*, Phys. Rev. C **46**, R1577 (1992).

[22] X. Lopez *et al.*, Phys. Rev. C **76**, 052203(R) (2007); A. Andronic *et al.*, Phys. Lett. B **612**, 173 (2005); H. H. Gutbrod *et al.*, Z. Phys. A **337**, 57 (1990); A. Andronic *et al.*, Nucl. Phys. A **679**, 765 (2001); J. Lukasik *et al.*, Phys. Lett. B **608**, 223 (2005); (INDRA Collaboration), presented at the International Workshop on Multifragmentation and Related Topics (IWM2003), Caen, France, 2003 (unpublished).

[23] C. Roy *et al.*, Z. Phys. A **358**, 73 (1997).